




Title	Biosynthesis of poly(glycolate-co-3-hydroxybutyrate-co-3-hydroxyhexanoate) in Escherichia coli expressing sequence-regulating polyhydroxyalkanoate synthase and medium-chain-length 3-hydroxyalkanoic acid coenzyme A ligase
Author(s)	Tomita, Hiroya; Satoh, Keigo; Nomura, Christopher T; Matsumoto, Ken'ichiro
Citation	Bioscience, Biotechnology, and Biochemistry, 86(2), 217-223 https://doi.org/10.1093/bbb/zbab198
Issue Date	2022-02
Doc URL	http://hdl.handle.net/2115/83966
Rights	© The Author(s) 2021. Published by Oxford University Press on behalf of Japan Society for Bioscience, Biotechnology, and Agrochemistry.
Type	article
File Information	zbab198.pdf



[Instructions for use](#)

REGULAR PAPER

Biosynthesis of poly(glycolate-co-3-hydroxybutyrate-co-3-hydroxyhexanoate) in *Escherichia coli* expressing sequence-regulating polyhydroxyalkanoate synthase and medium-chain-length 3-hydroxyalkanoic acid coenzyme A ligase

Hiroya Tomita ¹, Keigo Satoh,² Christopher T. Nomura,³ and Ken'ichiro Matsumoto^{1,*}

¹Division of Applied Chemistry, Faculty of Engineering, Hokkaido University, Kitaku, Sapporo, Japan;

²Graduate School of Chemical Sciences and Engineering, Hokkaido University, Kitaku, Sapporo, Japan; and

³Department of Biological Sciences, University of Idaho, Moscow, ID, USA

*Correspondence: Ken'ichiro Matsumoto, mken@eng.hokudai.ac.jp

ABSTRACT

Chimeric polyhydroxyalkanoate synthase PhaC_{AR} is characterized by the capacity to incorporate unusual glycolate (GL) units and spontaneously synthesize block copolymers. The GL and 3-hydroxybutyrate (3HB) copolymer synthesized by PhaC_{AR} is a random-homo block copolymer, poly(GL-*ran*-3HB)-*b*-poly(3HB). In the present study, medium-chain-length 3-hydroxyhexanoate (3HHx) units were incorporated into this copolymer using PhaC_{AR} for the first time. The coenzyme A (CoA) ligase from *Pseudomonas oleovorans* (AlkK) serves as a simple 3HHx-CoA supplying route in *Escherichia coli* from exogenously supplemented 3HHx. NMR analyses of the obtained polymers revealed that 3HHx units were randomly connected to 3HB units, whereas GL units were heterogeneously distributed. Therefore, the polymer is composed of 2 segments: P(3HB-co-3HHx) and P(GL-co-3HB-co-3HHx). The thermal and mechanical properties of the terpolymer indicate no contiguous P(3HB) segments in the material, consistent with the NMR results. Therefore, PhaC_{AR} synthesized the novel block copolymer P(3HB-co-3HHx)-*b*-P(GL-co-3HB-co-3HHx), which is the first block polyhydroxyalkanoate copolymer comprising 2 copolymer segments.

Received: 9 October 2021; Accepted: 4 November 2021

© The Author(s) 2021. Published by Oxford University Press on behalf of Japan Society for Bioscience, Biotechnology, and Agrochemistry. All rights reserved. For permissions, please e-mail: journals.permissions@oup.com

Graphical Abstract



A novel terpolymer P(GL-co-3HB-co-3HHx) was produced using PCT and AlkK for monomer supply and PhaCAR for polymerization in *Escherichia coli*.

Keywords: polyhydroxyalkanoate, block copolymer, glycolate, 3-hydroxyhexanoate

Polyhydroxyalkanoates (PHAs) are bacterial storage polyesters that can be produced from various renewable biomass and used as plastic materials (Zhang et al. 2018; Bedade, Edson, and Gross 2021). PHA synthase (PhaC) plays a central role in the biosynthetic pathway of PHAs (Rehm 2003). PhaC is typically specific to 3-hydroxyacyl-coenzyme A (CoA) substrates (Sudesh, Abe and Doi 2000; Steinbüchel and Hein 2001) and synthesizes homopolymers and/or random copolymers, which have no regulated monomer sequence, with multiple monomer substrates (Doi, Kitamura and Abe 1995; Bartels et al. 2020).

Sequence-regulating PhaC is a recently discovered type of enzyme which is capable of spontaneously synthesizing block copolymers without the manipulation of feedstocks during cultivation (Matsumoto et al. 2018). PhaCAR, which is a unique sequence-regulating PHA synthase, is an engineered chimeric enzyme composed of PHA synthases from *Aeromonas caviae* and *Ralstonia eutropha* (*Cupriavidus necator*) (Matsumoto et al. 2009). Notably, PhaCAR possesses unusual substrate specificity toward glycolyl (GL)-CoA (Arai et al. 2020). We previously reported that PhaCAR synthesized a block copolymer of GL and 3-hydroxybutyrate (3HB), poly(GL-ran-3HB)-b-poly(3HB).

GL-based polymers are characterized by their high hydrolytic degradability. For example, chemically synthesized polyglycolic acid (PGA) and poly(lactide-co-glycolide) (PLGA) can be hydrolyzed without the action of esterases (Pandita, Kumar and Lather 2015). Such hydrolytically degradable polymers have the potential to undergo hydrolysis in animal tissues; thus, they have the potential to serve as rapidly bioabsorbable materials (Shawe et al. 2006; Pervaiz et al. 2019). In contrast, natural PHAs have low hydrolytic degradability and slow bioabsorption (Basnett et al. 2018; Chen and Zhang 2018). GL-based PHAs potentially exhibit an intermediate hydrolytic degradability between chemically prepared GL-based polymers and natural PHAs. In fact, the first GL-based PHA random copolymer P(GL-co-3HB) synthesized using PhaC1_{PS}STQK hydrolyzes in the absence of PHA depolymerases (Matsumoto et al. 2011, 2017).

P(GL-ran-3HB)-b-P(3HB) synthesized by PhaCAR contains 23 mol% GL, which is higher than that of PhaC1_{PS}STQK (16 mol%) obtained under the same culture conditions (Arai et al. 2020). The block copolymer contains a GL-rich segment with a local GL fraction of 71 mol%, indicating the superior GL-incorporating capacity of PhaCAR. However, a drawback of P(GL-ran-3HB)-b-P(3HB) is

the stiff and brittle properties of the produced material. A potentially effective strategy to improve the material properties of PHA is the incorporation of 3-hydroxyhexanoate (3HHx) units into the polymer. A successful example is P(3HB-co-3HHx), also known as PHBH (Sato et al. 2015), which exhibits higher flexibility than P(3HB) (Wong et al. 2012). Here, we report the incorporation of 3HHx as the third monomer into the copolymer with GL and 3HB repeating units by PhaCAR to improve the physical properties. Analysis of the structure and physical properties of the obtained polymer indicated that they are representative of a new GL-based block terpolymer with transparent and superior extensible properties.

To supply 3HHx-CoA, 3-hydroxyacyl-CoA ligase from *Pseudomonas oleovorans* (AlkK) (Wang et al. 2012) was utilized. In PHA-producing *Pseudomonas* strains, the enzyme serves as a *de novo* medium-chain-length (MCL) monomer-supplying pathway together with the 3-hydroxyacyl-acyl carrier protein thioesterase (PhaG) (Rehm, Krüger and Steinbüchel 1998; Wang et al. 2012). The *alkK* gene is functionally expressed in *Escherichia coli* (Satoh et al. 2005). Heterologous expression of PhaG and AlkK in *E. coli* enables the synthesis of MCL PHA from nonfatty acid carbon sources (Tappel et al. 2014; Scheel et al. 2019). In the present study, we utilized AlkK to supply 3HHx-CoA from exogenous 3HHx supplemented into the medium. This enzyme serves as an easy-to-use 3HHx-CoA supplying route in *E. coli*.

Materials and methods

Plasmid construction for polymer production

A plasmid for synthesizing P(GL-co-3HB-co-3HHx) was constructed based on pBSP_{Re}phaCAR_{pct} (Matsumoto et al. 2018). An *Afl*III recognition site was introduced downstream of the *pct* gene. Using this site, *alkK* from *P. oleovorans*, which encodes acyl-CoA ligase, was introduced. The resulting plasmid pBSP_{Re}phaCAR_{pctalkK} was confirmed not to possess any unintended mutations.

Preparation of 3HHx

Ethyl (R,S)-3-hydroxyhexanoate was hydrolyzed by adding an excess amount of 10 N NaOH on ice until the solution was no longer

phase separated. The solution was acidified to approximately pH 2 by adding 6 N HCl, and diethylether was then added to extract 3-hydroxyhexanoic acid. Diethylether was removed *in vacuo*, and the residues were dissolved in water and neutralized by NaOH to give sodium 3HHx (3HHx-Na) solution.

Polymer production and analysis

E. coli JM109 was used as the host for plasmid construction and polymer production. *E. coli* was cultivated in 1.5 mL Luria Bertani medium (10 g L⁻¹ NaCl, 5 g L⁻¹ yeast extract, and 10 g L⁻¹ tryptone) containing ampicillin (100 mg L⁻¹) at 30 °C for 12 h as the seed culture. For polymer production, cells harboring the plasmid for polymer production were cultivated at 30 °C for 48 h. As monomer precursors, 3HB-Na, GL-Na, and 3HHx-Na were added at 1.25 or 2.5, 2.5 or 5.0, and 0-2.5 g L⁻¹, respectively. The polymer content and monomer composition were analyzed by gas chromatography as described previously (Taguchi *et al.* 2008). The polymer used for subsequent analysis was extracted from cells at 12 or 24 h cultivation. The intracellular polymer in lyophilized cells was extracted using chloroform at 60 °C for 48 h.

¹H NMR and ¹³C NMR analyses of the extracted polymer in CDCl₃ were carried out as described previously (Arai *et al.* 2020). The molecular weight of the polymer was measured by size exclusion chromatography using polystyrene standards for calibration, as described previously (Arai *et al.* 2020).

Preparation of solvent-cast films and mechanical properties analysis

Solvent-cast films of the purified polymers were prepared as follows: Approximately 400 mg of purified polymer was dissolved in 10 mL of chloroform. The solution was then placed in a glass Petri dish, which was covered with aluminum foil with 10 holes ($\phi \sim 1$ mm), and placed on a horizontal table at room temperature to allow the solution to evaporate. After 2 weeks, the obtained circular film was further dried *in vacuo* for 24 h to remove any residual solvent. The resulting films were stored at room temperature for at least 2 more weeks prior to testing.

The tensile strength, Young's modulus, and elongation to break of the films were determined using a tensile testing machine (EZ-test, Shimadzu, Japan) operated at a tensile speed of 3 mm min⁻¹ at room temperature. Samples were cut from the films using a dumbbell-shaped cutter SDMP-1000-D (Dumbbell, Japan), with a gauge length and width of 12 and 2 mm, respectively.

Thermal properties analysis

The glass transition temperature (T_g) and melting temperature (T_m) of the synthesized polymers were analyzed by differential scanning calorimetry (DSC) analysis using DSC-8500 (PerkinElmer). Approximately 5-10 mg of each polymer was confined in an aluminum pan using a pressing machine (Mettler Toledo). Measurement was performed under nitrogen atmosphere (flow rate: 100 mL min⁻¹) at the following temperature control: (1) cooling from 30 to -30 °C at 50 °C min⁻¹, (2) cooling from -30 to -50 °C at 20 °C min⁻¹, (3) heating from -50 to 210 °C at 20 °C min⁻¹, (4) cooling from 210 to -30 °C at 50 °C min⁻¹, (5) cooling from -30 to -50 °C at 20 °C min⁻¹, (6) isothermal heating at -50 °C for 5 min, and (7) heating from -50 to 210 °C at 20 °C min⁻¹.

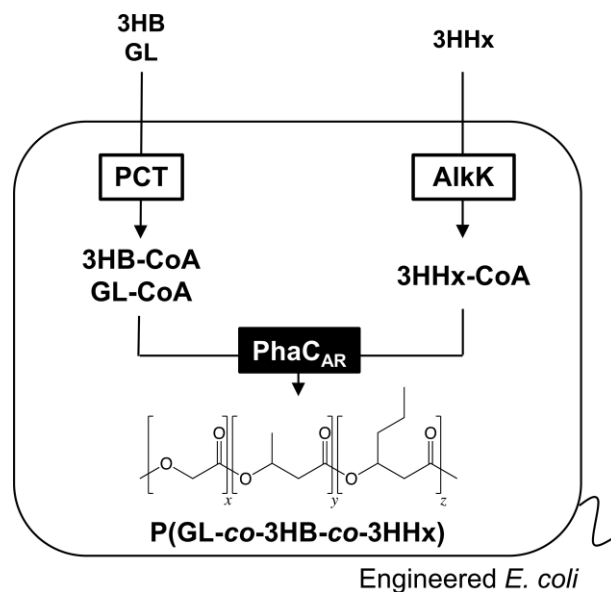


Figure 1. Illustration of the metabolic pathway used in this study to synthesize the terpolymer P(GL-co-3HB-co-3HHx) in *E. coli*. Propionyl-CoA transferase (PCT) transfers CoA from acetyl-CoA to GL and 3HB, thereby producing GL-CoA and 3HB-CoA. Acyl-CoA ligase (AlkK) is an ATP-dependent enzyme that activates 3HHx into 3HHx-CoA. PhaC_{AR} polymerizes the CoA thioesters.

Results and discussion

Biosynthesis of GL-based PHAs containing 3HHx units

The metabolic pathway used to synthesize PHAs containing GL, 3HB, and 3HHx is shown in Figure 1. GL, 3HB, and 3HHx were supplemented to the medium and taken up by *E. coli* cells. Propionyl-CoA transferase (PCT) derived from *Megasphaera elsdenii* converts GL and 3HB to GL-CoA and 3HB-CoA, respectively, using acetyl-CoA as a CoA donor. Acyl-CoA ligase (AlkK) activates 3HHx using ATP and free CoA to produce 3HHx-CoA (Wang *et al.* 2012).

First, we carried out polymer production with various concentrations of 3HHx-Na and fixed concentrations of GL-Na and 3HB-Na (Table 1). In this way, we successfully incorporated 3HHx into the copolymers. The supplemented 3HHx-Na was increased to 2 g L⁻¹, resulting in a subsequent increase in the 3HHx content but a decrease in the relative ratio of GL content within the copolymer (Table 1, Nos. 1-4). The 3HB fraction incorporated into the copolymers remained nearly constant despite the changing ratios of the other feedstocks. On the other hand, the cell dry weight (CDW) decreased as the 3HHx-Na concentration increased, particularly at concentrations above 2 g L⁻¹, suggesting that 3HHx inhibits cell growth (No. 5). In contrast, no significant changes in PHA production were observed. When we attempted polymer production in the absence of AlkK, the incorporation of 3HHx decreased compared to that in the presence of AlkK (Table S1). This result clearly demonstrates that AlkK plays an important role in providing 3HHx-CoA for polymer production.

Sequence analysis of 3HHx units

Due to the sequence-regulating capacity of PhaC_{AR}, the monomer sequence of the obtained polymer was of interest. Thus, the monomer sequence was analyzed based on changes in NMR chemical shifts influenced by the chemical structures of the adjacent units. The linkages between the 3HB and 3HHx units were determined by the ¹³C NMR resonances of carbonyl carbons. As shown in Figure 2 and Figure S1, 3 signals, which

Table 1. Synthesis of the GL-based polymers containing 3HHx

No.	Precursor Conc. ^a (g L ⁻¹)				Polymer production (g L ⁻¹)	Monomer composition (mol%)			Local GL fraction (mol%)	Molecular weight		
	GL	3HB	3HHx	CDW (g L ⁻¹)		GL	3HB	3HHx		M _n (× 10 ⁴)	M _w (× 10 ⁴)	M _w /M _n
1	2.50	2.50	0.00	3.75 ± 0.11	0.37 ± 0.03	27	73	0	68	2.6	5.4	2.1
2			0.50	3.28 ± 0.23	0.37 ± 0.07	17	68	15	56	6.9	9.9	1.4
3			1.00	3.15 ± 0.20	0.45 ± 0.07	9	64	27	30	6.5	15	2.3
4			1.50	2.45 ± 1.22	0.37 ± 0.14	5	59	36	- ^b	13	21	1.6

^aConcentrations of precursors are shown as sodium salts.

^bThe local GL fraction of 4 could not be calculated due to the low signal intensity. CDW: cell dry weight; M_w: weight average molecular weight; M_n: number average molecular weight; -: not tested due to poor cell growth. Values are the average ± SD of data from 3 independent experiments.

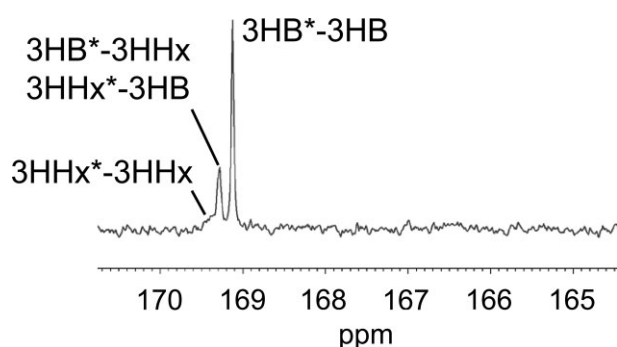


Figure 2. ¹³C NMR spectrum of polymer 2. Peaks correspond to the indicated dyads. GL-containing dyad peaks appear at δ 165–167. The overall spectrum is shown in Figure S1.

are ascribed to the carbonyl group of 3HB and 3HHx, were observed at δ 169.0–170.0. These 3 signals correspond to the dyad sequences of 3HHx*-3HHx, 3HB*-3HHx or 3HHx*-3HB, and 3HB*-3HB, respectively (Shimamura et al. 1994; Phithakrotchanakoon et al. 2015). Here, the asterisk indicates the focused unit of which the signal was observed. The abundant 3HB-3HHx/3HHx-3HB linkages indicate that 3HHx units were randomly incorporated into the polymer chain.

The resonances of the carbonyl carbon of the GL units were observed as split peaks in the range of δ 165.0–167.0 due to the triad sequence including GL units (Matsumoto et al. 2011, 2017). However, for the spectrum for polymer 2 which contains 17 mol% GL, the resonance of GL units was not clearly observed due to the low signal intensity. In addition, as GL has a short main-chain, its resonance can be subject to be influenced by the adjacent monomer units. The signal of the carbonyl carbon of GL is predicted to be divided into 9 triad patterns (3HB/3HHx/GL-GL*-3HB/3HHx/GL), therefore the intensity could be very weak to be detected. Indeed, for another terpolymer harboring 19 mol% GL, the signals were slightly observed (Figure S2).

Sequence analysis of GL units

Previous research has demonstrated that the ¹H NMR resonance of the methylene proton of GL in P(GL-*ran*-3HB) is observed as 4 characteristic signals at Δ4.5–4.9 ppm, which are ascribed to GL-GL*-GL (a), GL-GL*-3HB or 3HB-GL*-GL (b) or (c), and 3HB-GL*-3HB (d) triad sequences, respectively (Figure 3) (Arai et al. 2020; Matsumoto et al. 2017). Similarly, the terpolymer exhibits 4 similar signals that correspond to GL-GL*-GL (a), GL-GL*-3HB/3HHx or 3HB/3HHx-GL*-GL (b) or (c), and 3HB/3HHx-

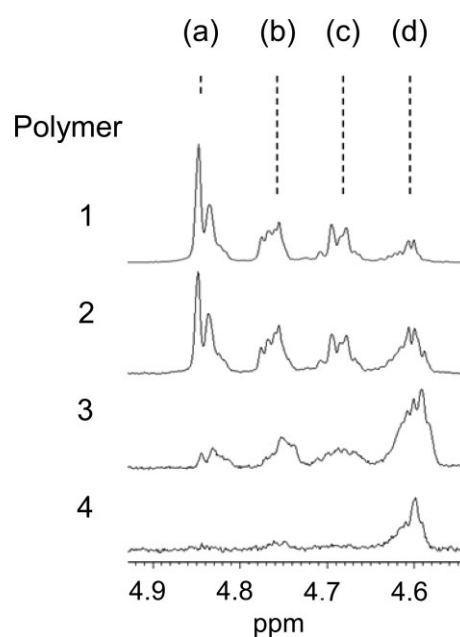


Figure 3. Partial ¹H NMR spectra of polymers 1–4. Peaks (a)–(d) correspond to the monomer triads: GL-GL*-GL (a), GL-GL*-(3HB/3HHx) and (3HB/3HHx)-GL*-GL (b) or (c), and (3HB/3HHx)-GL*-(3HB/3HHx) (d), respectively. The full spectra are shown in Figure S3.

GL*-(3HB/3HHx) (d), respectively (Figure S3). The effects of 3HB and 3HHx units in the triads on the chemical shift of the GL proton were indistinguishable. Based on the relative intensities of the 4 signals, the local GL fraction, which is defined as the molar ratio of GL units in a segment of P(GL-co-3HB) (Arai et al. 2020), can be calculated (Table 1 and Table S2). In our previous study, for example, we found that P(40 mol% GL-co-3HB) has a GL-rich segment in which the local GL fraction is estimated to be 71 mol% (Arai et al. 2020). Here, we calculated the local GL fraction of the terpolymer in the same way (Table 1 and Table S2). In all of the polymers produced and analyzed, the local GL fractions were higher than the total GL fractions, clearly indicating the heterogeneous distribution of GL units in the polymer chain. For polymer 1 P(GL-co-3HB), the resonance pattern was similar to that in our previous study (Arai et al. 2020). The intensity of (a) (a in Table S2) was the highest among the 4 signals, followed by b and c, and d was the lowest (Table S2). This result demonstrates that the GL-rich segment is present in polymer 1. For polymers 2–4, as the 3HHx fraction increased, a–c decreased whereas d increased. The local GL fraction of polymer 2 was 56 mol%

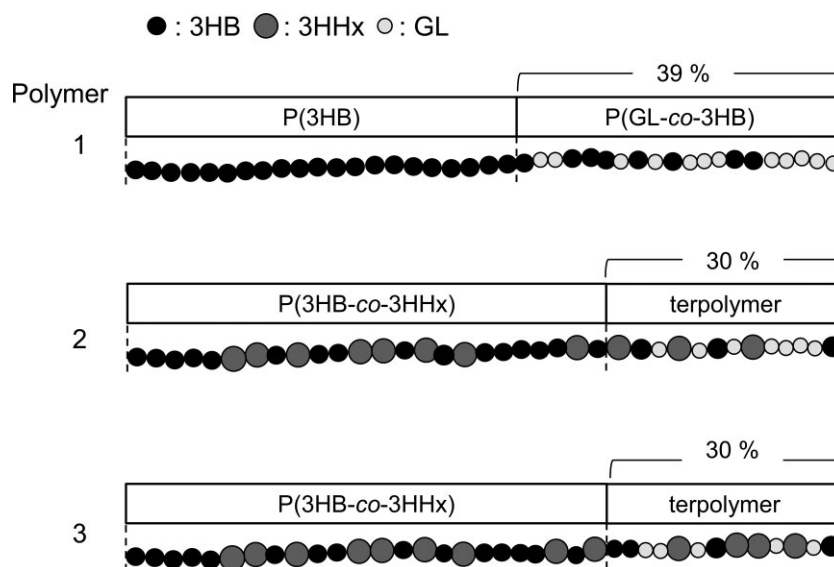


Figure 4. Proposed sequence structures of P(GL-co-3HB-co-3HHx) synthesized using PhaCAR. The number and the order of the segments are not determined.

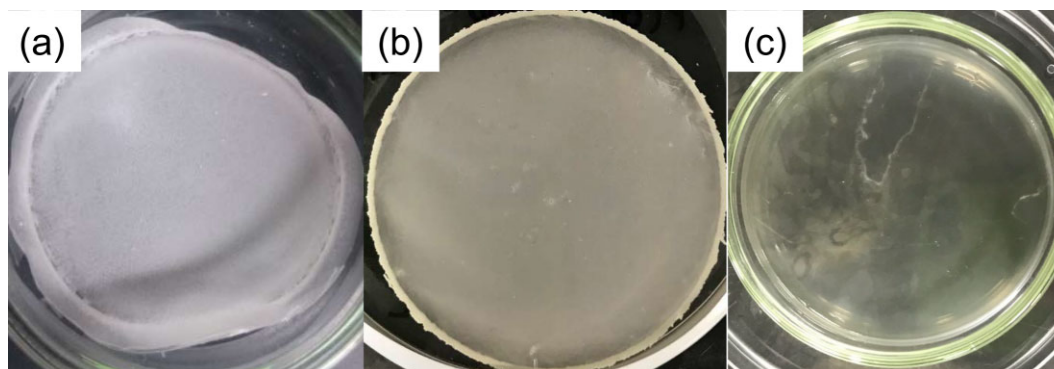


Figure 5. The appearance of the solvent-cast films. (a) P(20 mol% GL-co-3HB) (Arai *et al.* 2020), (b) P(17 mol% GL-co-3HB-co-15 mol% 3HHx) (2), and (c) P(9 mol% GL-co-3HB-co-27 mol% 3HHx) (3).

(Table 1). The ratio of the GL-rich segment in 1 was estimated to be 39%, which is higher than that in 2 and 3 (30%), whereas the ratio and the local GL fraction of 4 could not be determined due to its low signal intensity of GL units. Therefore, the ratio of the GL-rich segment was reduced by the incorporation of 3HHx.

Based on the results of NMR analysis, we propose the polymer structures (Figure 4). The structure for polymer 1 is similar to that observed in our previous study, which is P(GL-*ran*-3HB)-*b*-P(3HB) (Arai *et al.* 2020). For polymer 2, the ^{13}C NMR results suggest the presence of a P(3HB-co-3HHx) segment while ^1H NMR suggests the presence of a terpolymer segment. Thus, 2 can be presumed to be P(3HB-co-3HHx)-*b*-P(GL-co-3HB-co-3HHx). The monomer sequence in each segment is presumably random, although the statistical randomness in the terpolymer segment cannot be determined from the obtained data. For polymer 4, the GL-rich segment disappeared; thus, it is presumed to be P(GL-co-3HB-co-3HHx).

It should be noted that the current analysis does not determine the number and the order of the segments. Figure 4 depicts the total amount (ratio) of each segment, but does not necessarily mean that the obtained polymer is a diblock copolymer.

Mechanical properties of solvent-cast films

The solvent-cast film of P(20 mol% GL-co-3HB) (Arai *et al.* 2020) was opaque due to the high crystallinity of P(3HB), whereas those of polymers 2 and 3 were transparent (Figure 5). These results suggest that the incorporation of 3HHx lowers the crystallinity of the polymers. Next, stress-strain tests were carried out on the films at room temperature (Figure S4 and Table 2). The Young's modulus of polymers 2 and 3 (P(GL-co-3HB-co-3HHx)) was much lower than that of 1 (P(GL-co-3HB)) and PHBH, indicating that the terpolymer is a very soft and extensible material.

Thermal properties of the polymers

The thermal properties of the synthesized polymers were determined (Figure 6 and Table 3). Polymer 1 exhibited a melting peak at 157.6 °C, which can be ascribed to the relatively large crystalline fraction of P(3HB). For the polymers containing 3HHx, as the 3HHx fraction increased, the area of the melting peak decreased and eventually disappeared. This result indicates that the incorporation of 3HHx units drastically lowered the crystallinity of the polymer, and that the P(3HB) homopolymer segment does not exist in polymers 2-4. This finding is

Table 2. Mechanical properties of GL-based PHAs

No.	Film composition	Tensile strength (MPa)	Young's modulus (MPa)	Elongation to break (%)
- ^a	P(20 mol% GL-co-3HB)	16	348	7
2	P(17 mol% GL-co-3HB-co-15 mol% 3HHx)	1.3	63	8
3	P(9 mol% GL-co-3HB-co-27 mol% 3HHx)	1.0	7.2	43

^aThis polymer was synthesized and reported in our previous study (Arai et al. 2020).

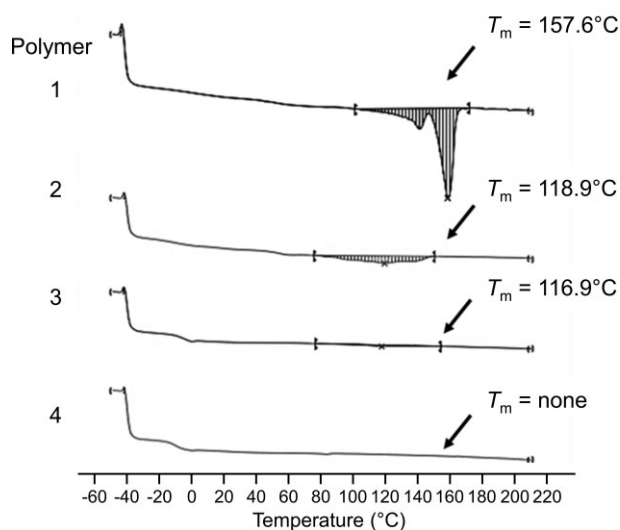


Figure 6. DSC analysis of the synthesized polymers.

Table 3. Thermal properties of the synthesized polymers

Polymer	Monomer composition (mol%)			T_g (°C)	T_m (°C)	ΔH (J g ⁻¹)
	GL	3HB	3HHx			
1	27	73	0	-0.6	157.6	43.5
2	17	68	15	-2.5	118.9	21.3
3	9	64	27	-5.2	116.9	2.3
4	5	59	36	-10.5	ND	ND

ND: not detected.

consistent with appearance and physical properties of the solvent-cast films described above and further supports the proposed structures shown in Figure 4.

Conclusion

The sequence-regulating PHA synthase PhaC_{AR} synthesized a novel GL-based terpolymer P(3HB-co-3HHx)-b-P(GL-co-3HB-co-3HHx), which is the first PHA block copolymer composed of 2 random copolymer segments. An inverse relationship was observed between GL and 3HHx fractions. In addition, the ratio of GL-containing segments was reduced by introducing 3HHx units. However, the mechanism of this phenomenon at the molecular level remains unclear. To achieve the combination of hydrolytic degradability and flexible properties, a greater ratio of GL-rich segments containing 3HHx units is preferable. Therefore, further improvement of the biosynthetic system is needed. The hydrolytic degradability and bioabsorption of the terpolymer and P(GL-co-3HB) synthesized using PhaC1_{P8}STQK will be addressed in our future work.

Supplementary material

Supplementary material is available at [Bioscience, Biotechnology, and Biochemistry](#) online.

Data availability

The data underlying this article are available in the article and in its online supplementary material.

Author contribution

H.T. analyzed data and wrote the manuscript. K.S. performed the experiments, analyzed data, and wrote the manuscript. C.N. provided the *alkK* gene and wrote the manuscript. K.M. designed and supervised this study, analyzed data, and wrote the manuscript. All authors read and approved the final version of the manuscript.

Funding

This work was supported by the JST-Mirai Program (No. JPMJMI19EB) and JSPS Kakenhi (20H04368).

Disclosure statement

No potential conflict of interest was reported by the authors.

References

- Arai S, Sakakibara S, Mareschal R et al. Biosynthesis of random-homo block copolymer poly[glycolate-*ran*-3-hydroxybutyrate (3HB)]-*b*-Poly(3HB) using sequence-regulating chimeric polyhydroxyalkanoate synthase in *Escherichia coli*. *Front Bioeng Biotechnol* 2020;8:612991.
- Bartels M, Gutschmann B, Widmer T et al. Recovery of the PHA copolymer P(HB-co-HHx) with non-halogenated solvents: influences on molecular weight and HHx-content. *Front Bioeng Biotechnol* 2020;8:944.
- Basnett P, Marcello E, Lukasiewicz B et al. Biosynthesis and characterization of a novel, biocompatible medium chain length polyhydroxyalkanoate by *Pseudomonas mendocina* CH50 using coconut oil as the carbon source. *J Mater Sci: Mater Med* 2018;29:179.
- Bedade DK, Edson CB, Gross RA. Emergent approaches to efficient and sustainable polyhydroxyalkanoate production. *Molecules* 2021;26:3463.
- Chen GQ, Zhang J. Microbial polyhydroxyalkanoates as medical implant biomaterials. *Artif Cells Nanomed Biotechnol* 2018;46:1-18.

- Doi Y, Kitamura S, Abe H. Microbial synthesis and characterization of poly(3-hydroxybutyrate-co-3-hydroxyhexanoate). *Macromolecules* 1995;**28**:4822-8.
- Matsumoto K, Hori C, Fujii R et al. Dynamic changes of intracellular monomer levels regulate block sequence of polyhydroxyalkanoates in engineered *Escherichia coli*. *Biomacromolecules* 2018;**19**:662-71.
- Matsumoto K, Ishiyama A, Sakai K et al. Biosynthesis of glycolate-based polyesters containing medium-chain-length 3-hydroxyalkanoates in recombinant *Escherichia coli* expressing engineered polyhydroxyalkanoate synthase. *J Biotechnol* 2011;**156**:214-7.
- Matsumoto K, Shiba T, Hiraide Y et al. Incorporation of glycolate units promotes hydrolytic degradation in flexible poly(glycolate-co-3-hydroxybutyrate) synthesized by engineered *Escherichia coli*. *ACS Biomater Sci Eng* 2017;**3**:3058-63.
- Matsumoto K, Takase K, Yamamoto Y et al. Chimeric enzyme composed of polyhydroxyalkanoate (PHA) synthases from *Ralstonia eutropha* and *Aeromonas caviae* enhances production of PHAs in recombinant *Escherichia coli*. *Biomacromolecules* 2009;**10**:682-5.
- Pandita D, Kumar S, Lather V. Hybrid poly(lactic-co-glycolic acid) nanoparticles: design and delivery prospectives. *Drug Discov Today* 2015;**20**:95-104.
- Pervaiz F, Ahmad M, Li L et al. Development and characterization of olanzapine loaded poly(lactide-co-glycolide) microspheres for depot injection: *in vitro* and *in vivo* release profiles. *Curr Drug Delivery* 2019;**16**:375-83.
- Phithakrotchanakoon C, Champreda V, Aiba S-I et al. Production of polyhydroxyalkanoates from crude glycerol using recombinant *Escherichia coli*. *J Polym Environ* 2015;**23**:38-44.
- Rehm BH. Polyester synthases: natural catalysts for plastics. *Biochem J* 2003;**376**:15-33.
- Rehm BH, Krüger N, Steinbüchel A. A new metabolic link between fatty acid *de novo* synthesis and polyhydroxyalkanoic acid synthesis. The PHAG gene from *Pseudomonas putida* KT2440 encodes a 3-hydroxyacyl-acyl carrier protein-coenzyme a transferase. *J Biol Chem* 1998;**273**:24044-51.
- Sato S, Maruyama H, Fujiki T et al. Regulation of 3-hydroxyhexanoate composition in PHBH synthesized by recombinant *Cupriavidus necator* H16 from plant oil by using butyrate as a co-substrate. *J Biosci Bioeng* 2015;**120**:246-51.
- Satoh Y, Murakami F, Tajima K et al. Enzymatic synthesis of poly(3-hydroxybutyrate-co-4-hydroxybutyrate) with CoA recycling using polyhydroxyalkanoate synthase and acyl-CoA synthetase. *J Biosci Bioeng* 2005;**99**:508-11.
- Scheel RA, Fusi AD, Min BC et al. Increased production of the value-added biopolymers poly(R-3-hydroxyalkanoate) and poly(γ -glutamic acid) from hydrolyzed paper recycling waste fines. *Front Bioeng Biotechnol* 2019;**7**:409.
- Shawe S, Buchanan F, Harkin-Jones E et al. A study on the rate of degradation of the bioabsorbable polymer polyglycolic acid (PGA). *J Mater Sci* 2006;**41**:4832-8.
- Shimamura E, Kasuya K, Kobayashi G et al. Physical properties and biodegradability of microbial poly(3-hydroxybutyrate-co-3-hydroxyhexanoate). *Macromolecules* 1994;**27**:878-80.
- Steinbüchel A, Hein S. Biochemical and molecular basis of microbial synthesis of polyhydroxyalkanoates in microorganisms. *Adv Biochem Eng Biotechnol* 2001;**71**:81-123.
- Sudesh K, Abe H, Doi Y. Synthesis, structure and properties of polyhydroxyalkanoates: biological polymers. *Prog Polym Sci* 2000;**25**:1503-55.
- Taguchi S, Yamada M, Matsumoto K et al. A microbial factory for lactate-based polyesters using a lactate-polymerizing enzyme. *Proc Natl Acad Sci USA* 2008;**105**:17323-7.
- Tappel RC, Pan W, Bergey NS et al. Engineering *Escherichia coli* for improved production of short-chain-length-co-medium-chain-length poly[(R)-3-hydroxyalkanoate] (SCL-co-MCL PHA) copolymers from renewable nonfatty acid feedstocks. *ACS Sustain Chem Eng* 2014;**2**:1879-87.
- Wang Q, Tappel RC, Zhu C et al. Development of a new strategy for production of medium-chain-length polyhydroxyalkanoates by recombinant *Escherichia coli* via inexpensive non-fatty acid feedstocks. *Appl Environ Microbiol* 2012;**78**:519-27.
- Wong YM, Brigham CJ, Rha C et al. Biosynthesis and characterization of polyhydroxyalkanoate containing high 3-hydroxyhexanoate monomer fraction from crude palm kernel oil by recombinant *Cupriavidus necator*. *Bioresour Technol* 2012;**121**:320-7.
- Zhang J, Shishatskaya EI, Volova TG et al. Polyhydroxyalkanoates (PHA) for therapeutic applications. *Mater Sci Eng C Mater Biol Appl* 2018;**86**:144-50.